EurJOC European Journal of Organic Chemistry

FULL PAPER

DOI: 10.1002/ejoc.201200836

Corrole–Porphyrin Conjugates with Interchangeable Metal Centers

Thien H. Ngo,[a,b] Francesco Nastasi,[c] Fausto Puntoriero,[c] Sebastiano Campagna,*[c] Wim Dehaen,[a] and Wouter Maes*[a,d]

Keywords: Porphyrinoids / Macromolecules / Energy transfer / Chromophores / UV/Vis spectroscopy

Oligoporphyrinoid materials composed of two or three tetrapyrrolic macrocycles have been synthesized by either mono- or disubstitution (S_NAr) of a phenolic Zn-AB_3-porphyrin on a *meso*-dichloropyrimidinyl-substituted Cu-AB_2-corrole. Selective metallation/demetallation sequences were carried out on these mixed corrole–porphyrin conjugates to afford multichromophoric systems with variable metal centers. The absorption spectra of the free-base corrole–porphyrin systems were essentially additive, which demonstrates that only weak intercomponent interactions take place in these assemblies and therefore they can be regarded as supramolecular systems. Photophysical studies of the free-base conjugates showed that these species are highly fluorescent, with fluorescence occurring from the lowest-energy singlet state of the porphyrin subunit(s), which is (are) the lowest-energy state(s) of the assemblies. Pump-probe transient absorption spectroscopy experiments demonstrated that very efficient (>95 %) corrole-to-porphyrin singlet–singlet energy transfer takes place in these pyrimidinyl-bridged multichromophoric systems by a coulombic mechanism with rate constants on the picosecond timescale.

Introduction

The investigation of corroles, contracted porphyrin analogues lacking one *meso*-carbon atom, dates back to the early 1960s when the first corrole synthesis was reported by Johnson and Kay.[1] For decades thereafter, however, corrole research has been overshadowed by porphyrin science, partly due to the challenging corrole synthesis. Recent increased interest in corrole-based materials and their applications is in great part due to the impressive synthetic progress that has been made in the field over the last 15 years,[2,3] and many studies now focus on the coordination chemistry or electrochemistry of diverse (metallo)corroles and their applications in sensors, catalysis, medicine, and molecular electronics.[4]

The integration of multiple corroles (and their combination with porphyrins) into larger macromolecular structures has scarcely been explored so far, although the potential of such conjugates in a number of applications can easily be seen. These systems may, for instance, be used as multisite catalysts, mimics of biochemically important species (e.g., cytochrome c oxidase), or optical sensors. Moreover, they are also appealing tools for gaining an understanding of the basic photophysical phenomena that occur in corroles and multiporphyrinoid structures en route towards their possible exploitation in molecular electronics and/or solar-energy conversion. To date, only a few corrole–porphyrin and corrole-corrole dyads have been prepared.[5–9] The traditional syntheses of mixed porphyrin–corrole derivatives have often involved either corrole synthesis starting from porphyrin-containing precursors or porphyrin synthesis starting from corrole-containing building blocks. The described procedures are often not very straightforward, requiring laborious multistep sequences and modifications at the porphyrinoid level, and the modest yields imply the loss of valuable (tetrapyrrolic) material. Bis-corrole systems linked through the 10-position with phenyl spacers have been prepared by Paolesse and co-workers through multistep sequences.[5] Guilard and co-workers synthesized a series of face-to-face bis-corroles and porphyrin–corrole dyads with different (rigid or flexible) linkers starting from dialdehyde linker precursors.[6] An atypical mixed macrocycle system from the same group involved a Rh-tetraphenylporphyrin–Sn-corrole dyad with a metal–metal bond.[6d]

[a] Molecular Design and Synthesis, Department of Chemistry, KU Leuven,
Celestijnenlaan 200F, 3001 Leuven, Belgium
[b] Institut für Chemie und Biochemie – Organische Chemie, Freie Universität Berlin,
Takustrasse 3, 14195 Berlin, Germany
[c] Dipartimento di Chimica Inorganica, Chimica Analitica e Chimica Fisica, Università di Messina and Centro Interuniversitario per la Conversione Chimica dell'Energia Solare (SOLAR-CHEM),
98166 Vill. S. Agata, Messina, Italy
Fax: +39-090-393756
E-mail: campagna@unime.it
[d] Design & Synthesis of Organic Semiconductors (DSOS), Institute for Materials Research (IMO-IMOMEC), Hasselt University,
Agoralaan 1, Building D, 3590 Diepenbeek, Belgium
Fax: +32-11-268299
E-mail: wouter.maes@uhasselt.be
Homepage: http://www.uhasselt.be/UH/IMO/Visit-the-groups/Design-and-synthesis-of-organic-semiconductors.html

Supporting information for this article is available on the WWW under http://dx.doi.org/10.1002/ejoc.201200836.

Osuka and Cavaleiro and their co-workers reported the synthesis of β,β′-linked corrole dimers by Suzuki–Miyaura cross-coupling (after regioselective Ir-catalyzed direct borylation) or simple heating of tris(pentafluorophenyl)corrole in 1,2,4-trichlorobenzene, respectively.[7a–7c] Gryko and co-workers prepared a stable corrole–porphyrin dyad by linking two preformed macrocycles through an amide bridge.[7d] The same group also reported *meso*,*meso*′-linked bis-corroles synthesized by cascade reactions of sterically hindered dipyrromethanes and formaldehyde (in low yields).[7e] Upon nitration of nonaromatic Ni-corroles with peripherally fused ring systems, obtained by ring contraction of nickel *meso*-tetraarylporphyrins, a series of β,β′-linked corrole dimers were synthesized by Callot and co-workers by electron-transfer-initiated coupling.[8,9]

Metallation of tetrapyrrolic dyads is generally not selective (with a few notable exceptions).[5–9] Upon desired metallation of the corrolato ligand, the same metal will often simultaneously insert into the porphinato ligand (albeit normally in a lower oxidation state). To achieve selective metallation of the individual tetrapyrrolic units within one dyad, of particular interest to create energy funneling pathways, the metals usually have to be inserted into the porphyrinoid building blocks prior to combining them, which considerably increases the effort required to obtain a variety of differently metallated systems for screening purposes.

From this literature survey, it is clear that novel synthetic pathways with enlarged versatility and scope (e.g., regarding the substitution pattern and metallation state) are highly desirable to achieve further progress in the field and to pursue realistic applications of such materials. The synthetic route presented herein enables straightforward access to either bis- or tris-porphyrinoid systems with different metal centers in each macrocyclic ligand starting from a single oligoporphyrinoid platform, readily available by combination of a phenolic AB_3-porphyrin and a *meso*-dichloropyrimidinyl-substituted AB_2-corrole. Absorption spectra and photophysical properties (both in fluid solution at room temperature and in a rigid matrix at 77 K) of selected compounds, that is, two free-base (Fb) corrole–porphyrin conjugates and their individual components, have also been investigated. The corrole-to-porphyrin energy-transfer processes occurring in such compounds have been analyzed by pump-probe transient absorption spectroscopy.

Results and Discussion

Synthesis of Corrole–porphyrin Conjugates

As described in previous work, the introduction of *meso*-pyrimidinyl groups at the periphery of triarylcorroles[10] (and analogous porphyrinoids[11]) allows a straightforward introduction of different (functional) moieties on to the tetrapyrrolic macrocycle by (post-macrocyclization) nucleophilic aromatic substitution (S_NAr) or Pd-catalyzed cross-coupling reactions. As such, pyrimidinylcorroles are versatile synthons towards more complex functional corrole materials. This functionalization approach can, in principle, also be extended to porphyrin and/or corrole substituents and, depending on the type of pyrimidinylcorrole (AB_2, A_2B, or A_3),[10] multiple porphyrinoid chromophores can be introduced on to the corrole framework. Combining this with a recently developed method that allows the smooth copper metallation and demetallation of the corrolato ligand,[12] multiple multichromophoric systems can be envisaged in which the porphyrin and corrole entities are equipped with different metal centers.

Lewis acid catalyzed (0.068 equiv. $BF_3{\cdot}OEt_2$) condensation of mesityldipyrromethane[13] with 4,6-dichloro-2-(methylsulfanyl)pyrimidine-5-carbaldehyde (1:1 ratio) afforded Fb-AB_2-pyrimidinylcorrole **1a** (27%), which was treated with copper acetate (in THF at room temp.) to yield the desired Cu-corrole scaffold **1b** (Scheme 1).[10a] As a nucleophilic porphyrinoid, phenolic AB_3-porphyrin **2a** was chosen due to its favorable solubilizing properties enabling easy synthetic routine handling and characterization of the final corrole–porphyrin conjugates. The peripheral porphyrin unit was prepared by a mixed Rothemund condensation of 3,5-di-*tert*-butylbenzaldehyde and 4-hydroxybenzaldehyde (2:1 ratio) with pyrrole.[11d,14] Subsequent metallation with zinc acetate (in $CHCl_3$ at room temp.) or platinum chloride (in benzonitrile at reflux) afforded Zn-porphyrin derivative **2b** and Pt-porphyrin **2c**, respectively (Scheme 1).[11d]

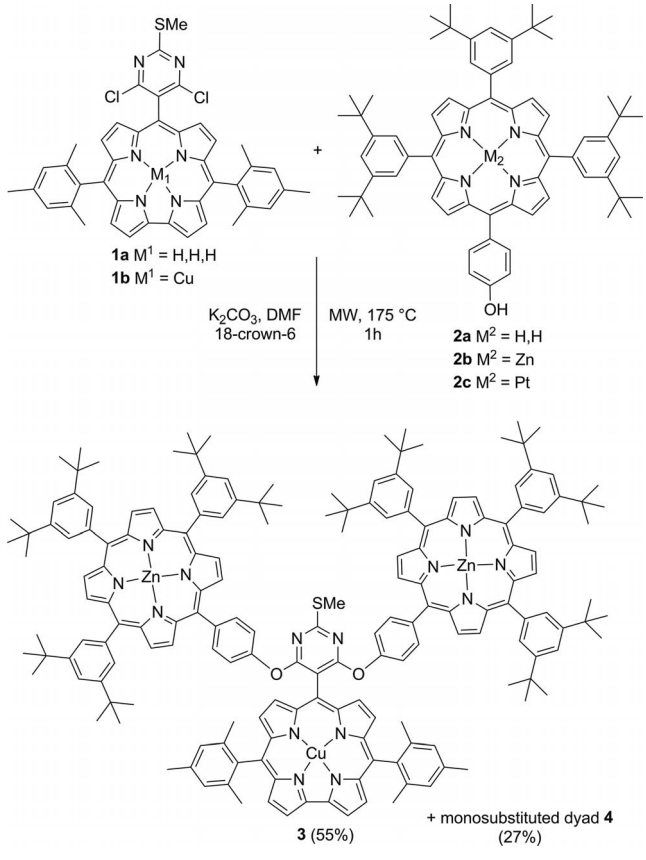

Scheme 1. Synthesis of the disubstituted conjugate **3** and the monosubstituted dyad **4**.

When Fb-pyrimidinylcorrole **1a** and an excess (6 equiv.) of Fb-porphyrin **2a** were treated under S_NAr conditions as optimized for AB_2-pyrimidinylcorroles (K_2CO_3, 18-crown-6, DMF, microwave, 175 °C, 1 h),[10a] a complex product mixture was obtained. Despite several purification attempts (column chromatography and preparative TLC on silica), none of the envisaged products could be obtained in pure form. To overcome this problem, which may be attributed to the relative (photo-oxidative) instability of the Fb-AB_2-pyrimidinylcorrole, the same reaction was carried out with Cu-corrole **1b** and Zn-porphyrin **2b**. After purification by column chromatography (silica), the disubstituted product **3** and monosubstituted analogue **4** were obtained in yields of 55 and 27%, respectively (Scheme 1). The excess (4 equiv.) of Zn-porphyrin **2b** could easily be recovered.

An additional advantage of *meso*-pyrimidinyl moieties is that the extent of substitution (mono/di) can be regulated to some extent by adjusting the reaction temperature.[10,11] When the same reaction was carried out at 90 °C (conventional heating) with only 1.5 equiv. of Zn-porphyrin **2b**, monosubstituted dyad **4** was obtained more selectively in 72% yield. Some of the starting Cu-corrole **1b** (10%) and the small excess of Zn-porphyrin **2b** could be recovered during the purification process.

Metallation/Demetallation Sequences

Corrole–porphyrin conjugates (and ultimately more elaborate corrole-based dendritic structures[11d,15,16]) are interesting photophysical probes in which the peripheral corrole and/or porphyrin moieties can act as light-absorbing antennae that transfer energy to a central porphyrinoid core. Suitable metal sites in the corrolato and porphinato ligands can have a major impact on the photophysical features of such systems. As mentioned above, the metals are usually introduced into each separate macrocycle before combining them into a multiporphyrinoid structure. Guilard and co-workers have reported the synthesis of cofacial heterodimetallic corrole–porphyrin dyads.[6] Cobalt metallation of the corrole moiety was performed on a Zn-porphyrin–Fb-corrole material.[6g] Alternatively, zinc and manganese were inserted into the porphyrin subunit of a Fb-porphyrin–Co-corrole dyad. The same group also reported the selective metallation of a fully Fb-corrole–porphyrin dyad.[6c] Cobalt could be inserted into the corrolato ligand [through the addition of $Co(OAc)_2$ in pyridine at 60 °C], but no insertion into the porphyrin moiety was observed. By raising the temperature to reflux, metallation of the porphyrin unit also occurred. However, when this procedure was repeated for a mixture of our precursors **1a** and **2a**, partial porphyrin metallation was observed by mass spectrometry (ESI-MS), even at room temperature. The same test experiment (metallation of a mixture of **1a** and **2a**) was carried out for aluminium ($AlMe_3$ in toluene at room temp.[17]) and platinum ($PtCl_2$ in benzonitrile at reflux[11d,18]). Partial Al insertion into Fb-porphyrin **2a** was observed, whereas decomposition of pyrimidinylcorrole **1a** occurred during the Pt insertion reaction.

A more general (ultimately orthogonal) strategy for obtaining variously metallated multiporphyrinoid systems can be established based on our earlier reported corrole Cu-metallation/demetallation cycle.[12c] Both procedures are mild and only require purification by flash column chromatography, minimizing decomposition. As described previously,[12c] Cu-pyrimidinylcorroles cannot be demetallated in acidic medium without a suitable reducing agent (e.g., $SnCl_2$). When Zn-porphyrin–Cu-corrole dyad **4** was treated with HCl in $CHCl_3$, the porphyrin entity was demetallated, whereas the Cu-corrole moiety remained untouched (Scheme 2). After purification by flash column chromatography, 78% of pure dyad **5** was obtained. Further copper demetallation of bis-porphyrinoid **5** was carried out under the optimized demetallation conditions and 63% of pure Fb-corrole-Fb-porphyrin dyad **6** was obtained (Scheme 2). Addition of zinc(II) acetate to a solution of conjugate **6** in $CHCl_3$ readily led to 87% of Zn-porphyrin–Fb-corrole **7**. Dyad **6** could also be prepared directly from fully metallated dyad **4** upon application of the optimized demetallation procedure for Cu-corroles. After purification, Fb conjugate **6** was isolated in an essentially quantitative yield (Scheme 2).

This concept was then extended to tris-porphyrinoid system **3** and other metal centers (Scheme 3). In this initial study, emphasis is on the proof-of-concept and metals were chosen for their easy insertion and/or resulting diamagnetism (towards NMR characterization) rather than for specific photophysical (absorption/luminescence) purposes. The same conditions as outlined above were applied to remove zinc from the porphyrin units. After purification, 63% of pure Fb-porphyrin–Cu-corrole conjugate **8** was obtained. Upon further application of the Cu-corrole demetallation procedure, full conversion to the Fb conjugate **9** was achieved in a nearly quantitative yield. Zinc was introduced into the two porphyrin moieties without simultaneous metallation of the corrole chromophore. After flash column chromatography, tris-porphyrinoid **10**, containing two Zn-porphyrins and a Fb-corrole, was isolated in nearly quantitative yield. Upon further metallation of the corrole moiety with gallium(III) trichloride (in pyridine at reflux),[19] Zn-porphyrin–Ga-corrole conjugate **11** was obtained in 76% yield. Complete direct demetallation starting from Zn-porphyrin–Cu-corrole **3** afforded the Fb derivative **9** in 75% yield.

When conjugate **8** was subjected to the metallation conditions generally applied to introduce platinum into a porphinato ligand ($PtCl_2$ in benzonitrile at reflux[18]), the desired Pt-porphyrin–Cu-corrole product **12** could not be obtained (Scheme 3). This was attributed to the decomposition of the Fb-porphyrin–Cu-corrole conjugate caused by the rather harsh metallation conditions or to the instability of the product **12**. After purification by column chromatography, only a very small amount (5%) of the starting material was recovered. Pt-porphyrin–Cu-corrole conjugates **12** and **13** were, however, obtained by carrying out the S_NAr reaction with Cu-corrole precursor **1b** and phenolic Pt-porphyrin **2c**. Disubstituted conjugate **12** was obtained in 73%

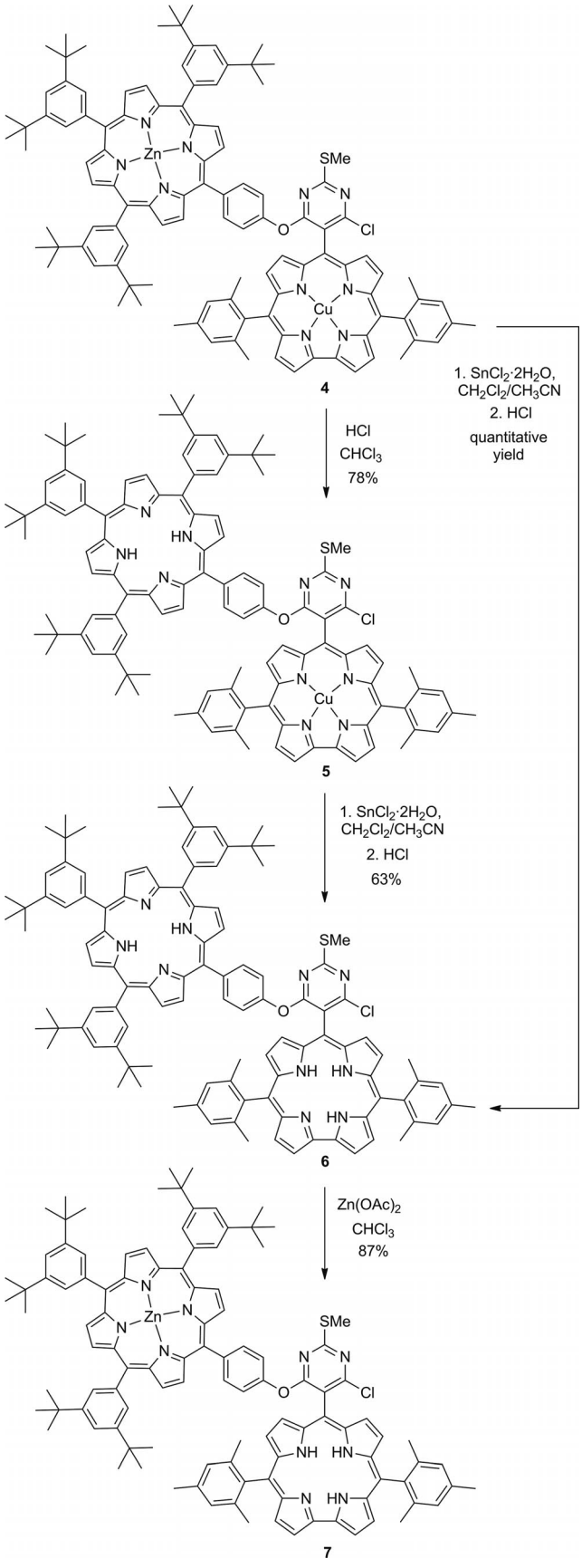

Scheme 2. Metallation/demetallation sequence for corrole–porphyrin dyad **4**.

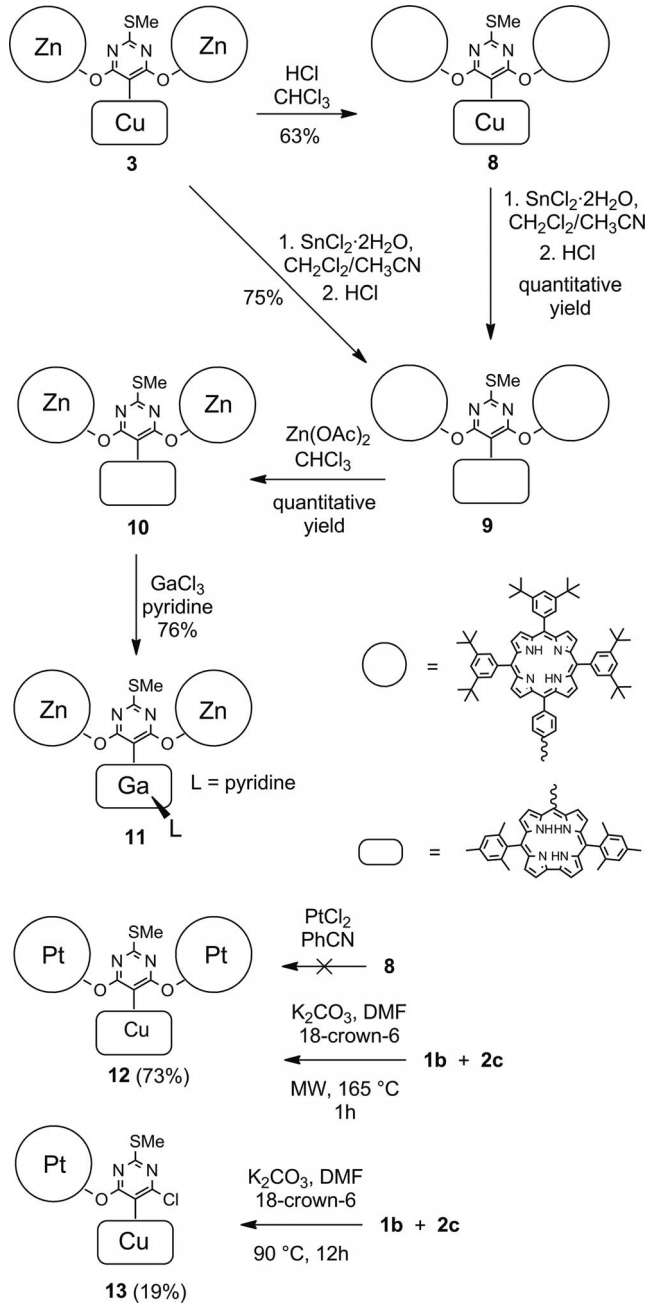

Scheme 3. Metallation/demetallation sequence starting from tris-porphyrinoid conjugate **3**.

yield by S_NAr reaction under microwave irradiation conditions. Selective monosubstitution was achieved by tuning the reaction conditions (90 °C) and monosubstituted conjugate **13** was obtained in 19% yield (Scheme 3). The low yield was again attributed to the decomposition of the product formed as a result of exposure to high temperature for a prolonged time (overnight).

Multichromophoric macromolecules **7** and **10** allow the introduction of different metals into the corrole core without exchanging the metals in the Zn-porphyrin moieties. When Zn is selectively removed from the peripheral porphyrin chromophores (in slightly acidic medium) and new

metals are inserted instead, novel combinations of metalloporphyrinoids can be envisaged. The opposite story can be told for Fb-porphyrin–Cu-corrole conjugates **5** and **8**, although the metalloporphyrin should be able to withstand the harsher conditions used to remove the Cu from the corrolato ligand in this case.

Absorption Spectra and Photophysical Properties

Because of the *ortho*,*ortho'*-di(hetero)aryl ether linkage(s) in the conjugates, the corrole and porphyrin moieties are positioned rather close in space. This could allow efficient interchromophoric interactions, in particular, photoinduced electronic energy transfer. As the excited-state energies of Fb-corroles are usually slightly higher than the excited-state energies of the corresponding Fb-porphyrins,[20] corrole-to-porphyrin energy transfer should occur. To investigate this topic, luminescence experiments were performed, both in fluid solution at room temperature and in a rigid matrix at 77 K, on the dyad **6** and the triad **9** (containing a Fb-corrole and one or two Fb-porphyrins, respectively). The properties of the porphyrin model compound **2a** have also been studied, whereas some data on the corrole model species **14** and **15** (Figure 1) are available from a former study[10b] and have been used here whenever necessary. All the important photophysical data are presented in Table 1. At this point the photophysical investigation was limited to the multichromophoric Fb species because our main interest was to study the eventual occurrence of intercomponent energy transfer in the pyrimidinyl-linked tetrapyrrolic conjugates. In fact, multichromophoric free bases **6** and **9** are the systems that allow clear-cut results instrumental to our aim on the basis of the luminescence properties of their individual components, in particular, the difference between their emission spectra.

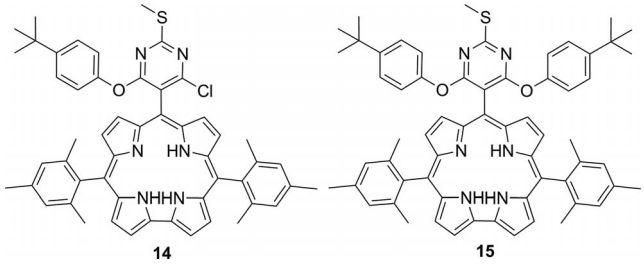

Figure 1. Pyrimidinylcorroles **14** and **15** used as model compounds in the photophysical studies.

The absorption spectra of the investigated compounds exhibit features typical of porphyrin and corrole compounds: Very intense Soret bands in the UV region and intense, structured Q-bands in the visible region. Figure 2 shows the absorption spectra of **2a**, **14**, **15**, **6**, and **9**, and relevant data are presented in Table 1. Note that the absorption spectra of the dyad and triad species are essentially the summation of the spectra of their model compounds (for example, compare the spectrum of **6** and the summation of the spectra of **2a** and **14**, Figure 2). This demonstrates that the electronic interaction between the corrole and porphyrin subunits in the multichromophoric species studied here is negligible and therefore these species can be regarded merely as supramolecular compounds. In particular, the bands in the 530–580 nm region in the absorption spectra of **6** and **9** receive significant independent contributions from the Q-bands of both the corrole and porphyrin subunits and the absorption in the 380–440 nm region receives independent contributions from the corrole and porphyrin Soret bands (Figure 2). The negligible electronic interaction between the corrole and porphyrin subunits in **6** and **9**, as inferred by the absorption spectra, contrasts with the non-negligible interaction between the chromophores in the so-called pacman-type corrole–porphyrin assemblies reported by Gros et al.,[6j] inferred also on the basis of the absorption spectra of the dyads and individual components. In the latter case, the face-to-face arrangement of the corrole and porphyrin subunits leads to a more intense interaction, whereas the less compact molecular structures of **6** and **9** apparently limit interchromophoric interactions, at least in the ground state.

The luminescence properties of model compound **2a** (Table 1) are in line with the general properties of standard tetraphenylporphyrins.[21] The emission has been assigned to fluorescence from the lowest-energy singlet state. Comparison with the luminescence properties of the corrole model species **14** and **15** (Figure 1, Table 1) indicates that energy transfer from the Fb-corrole unit to the Fb-porphyrin unit(s) in the multichromophoric systems **6** and **9** is thermodynamically allowed. The excited-state energy levels of the individual subunits are approximate to the higher-

Table 1. Absorption and luminescence properties of Fb conjugates **6** and **9** and their model species.[a]

	Absorption	Luminescence				
	λ_{max} [nm] (ε [$M^{-1}cm^{-1}$])	λ_{max} [nm] 298K	τ [ns] 298 K	Φ 298 K	λ_{max} [nm] 77 K	τ [ns] 77 K
2a	420 (420000), 515 (17000), 550 (9500), 590 (5000), 650 (4500)	655	10	0.11	655	13
6	420 (496000), 516 (28000), 555 (26300), 568 sh (23700), 600 (15700), 635 sh (5300), 650 (6400)	605,[b] 650	0.20,[c] 9	0.10	650	12
9	422 (691000), 517 (35000), 555 (25500), 593 (14300), 600sh (13700), 650 (8600)	605,[b] 650	0.12,[c] 10	0.10	650	12
14	410 (103000), 428 (90000), 570 (21300), 603 (10500), 634 (3100)	605sh, 645	4.2	0.098	600	7
15	410 (102100), 428 (91700), 571 (19300), 605 (10700), 637 (3100)	605sh, 645	5.9	0.152	602	12

[a] Data were recorded in air-equilibrated toluene, unless stated otherwise. [b] Very weak contribution, see onset of the emission spectra in Figure 3. [c] This component was only obtained by recording the lifetime in the 600–620 nm range.

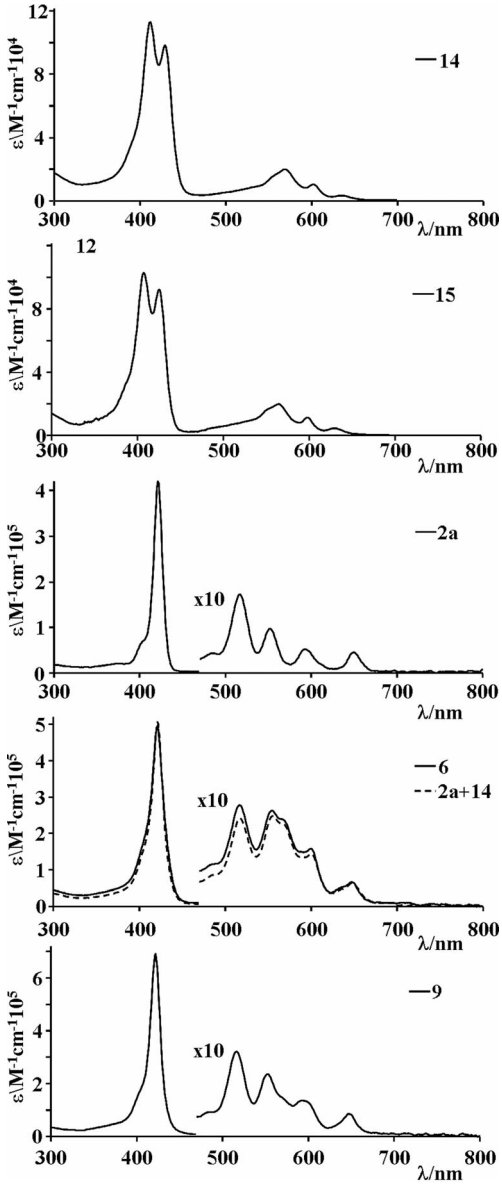

Figure 2. Absorption spectra (in toluene solution) of dyad **6**, triad **9**, and their model species. In the panel containing the spectrum of **6**, the spectrum **2a**+**14** is obtained by the sum of the individual spectra.

energy feature of the model emission band, which is located at about 605 nm for the corrole chromophores **14** and **15**, and at 655 nm for the porphyrin model species **2a**. With such an assumption, a driving force of around 0.15 eV was calculated for the corrole-to-porphyrin energy-transfer process. Indeed, both in fluid solution at room temperature and in a rigid matrix at 77 K (spectra not shown), the luminescence spectra of **6** and **9** are similar to those of **2a** (Figure 3; the comparison in intensity between the emission bands at 650 and 715 nm, due to vibrational progression, is particularly diagnostic). The luminescence lifetimes and quantum yields are also nearly identical to those of **2a** (Table 1) when experimental uncertainties are taken into account. These results indicate that quite efficient energy transfer from the higher-energy corrole singlet state to the lower-energy porphyrin singlet state takes place in the multichromophoric systems, both at room temperature in fluid solution and at 77 K in a rigid matrix. As additional confirmation of the energy-transfer process, note that the excitation spectra of **6** and **9**, recorded at 730 nm, closely resemble the respective absorption spectra, which clearly demonstrates that the light absorbed by the corrole subunit contributes to the (porphyrin-based) emission. The absorption and excitation spectra of dyad **6** are compared in Figure 4.

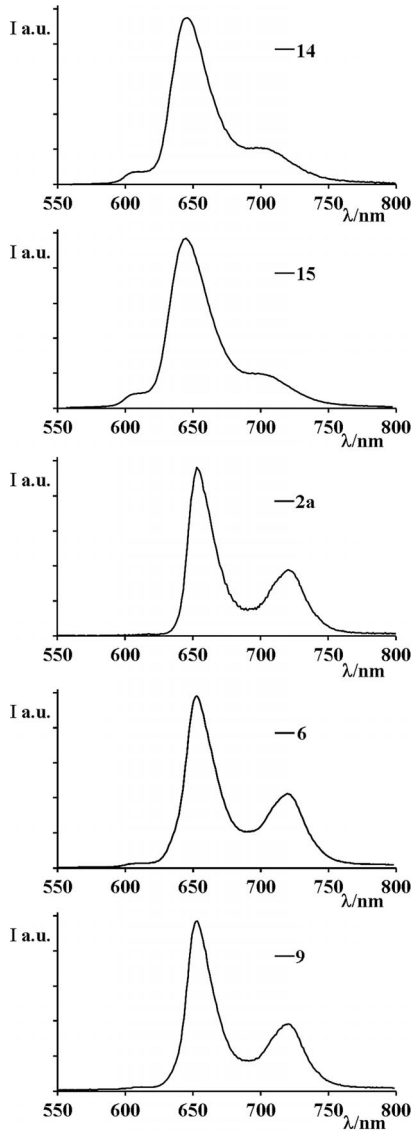

Figure 3. Luminescence spectra (in toluene solution at room temp.) of dyad **6**, triad **9**, and their model species.

A very small contribution to the emission spectra is present at about 605 nm in the emission spectra of **6** and **9** recorded at room temperature. On recording the emission lifetime at 610 nm, minor decay components appear with lifetimes of about 0.20 and 0.12 ns for **6** and **9**, respectively. In both cases, such a component can be assigned to the quenched corrole fluorescence in the dyad and triad species. By using such lifetimes and considering the fluorescence lifetimes of the model compounds **14** and **15** (4.2 and 5.9 ns,

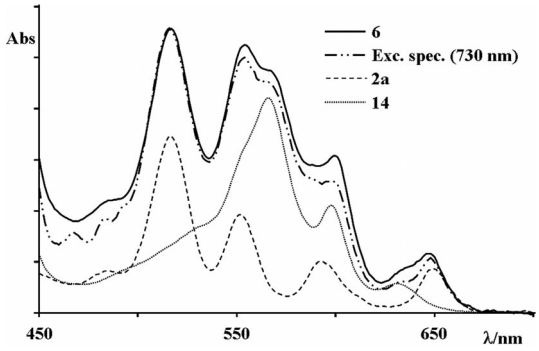

Figure 4. Comparison between the absorption (solid line) and excitation (dashed-dotted, emission wavelength 730 nm) spectra of the corrole–porphyrin dyad **6** in toluene at room temp. For completeness, the absorption spectra of the individual components **2a** (dashed) and **14** (dotted) are also shown. The absorption spectra are represented on the same molar absorption scale.

respectively; Table 1), energy-transfer rate constants of about 5×10^9 and 8×10^9 s^{-1} can be calculated for **6** and **9**, respectively [from the usual relationship $k_q = (1/\tau) - (1/\tau^0)$, in which k_q is the energy-transfer rate constant and τ and τ^0 are the fluorescence lifetimes of the corrole-based fluorescence in the quenched (i.e., **6** and **9**) species and the model systems]. These rates should, however, be considered with care as the measured lifetimes are close to the lower limit of our time-resolved luminescence equipment (ca. 100 ps, essentially due to the electronic delay of the instrument). Therefore the calculated energy-transfer rate constants are associated with some uncertainty. Nevertheless, from the luminescence experiments it can be concluded that for both conjugates **6** and **9** a highly efficient (>95%) corrole-to-porphyrin singlet–singlet energy transfer takes place.

To investigate the corrole-to-porphyrin energy-transfer processes occurring in the Fb conjugates in more detail, pump-probe transient absorption spectroscopy using femtosecond time resolution was performed. Figure 5 shows the transient absorption spectra (in toluene) of the parent chromophores **2a** and **14** and corrole–porphyrin conjugate **6** at room temperature (excitation wavelength 400 nm at 2 mJ). In the transient spectrum of monosubstituted corrole **14**, bleaching of the corrole absorption in the visible region is clearly apparent in the range 540–620 nm, although it is partially compensated by the presence of a transient absorption between 450 and 540 nm (Figure 5, top panel). Following a fast (few ps rate constant) initial process, mainly assigned to internal conversion and vibrational cooling, the transient absorption decays towards the ground state without showing any other spectral evolution. On the timescale used for pump-probe spectroscopy (3.2 ns), the ground state is not fully recovered (see inset of Figure 5, top panel; 517 nm decay). This finding is in agreement with the luminescence data, which indicate a lifetime of about 10 ns for the emissive lowest-energy singlet state of **14**. Note that, upon recording the kinetics of the bleaching recovery at 567 nm (Figure 5, top), besides the processes observed for the transient decay at 517 nm, a very long-living contribution is also present, most likely due to the triplet state of the corrole. It is indeed known that the triplet state of corroles appears as a constant bleach (on the ns timescale) in the 540–600 nm region.[20e] The transient absorption spectrum of **2a** (Figure 5, middle panel) is typical for porphyrin singlet states.[7d] An intense transient is clearly present in the visible region, which largely compensates for the bleaching of the Q-bands. Similarly to what happens for **14**, and in agreement with the luminescence data (Table 1), the transient spectrum of **2a** decays to the ground state on a longer timescale than the time limit of the equipment (see inset of Figure 5, middle).

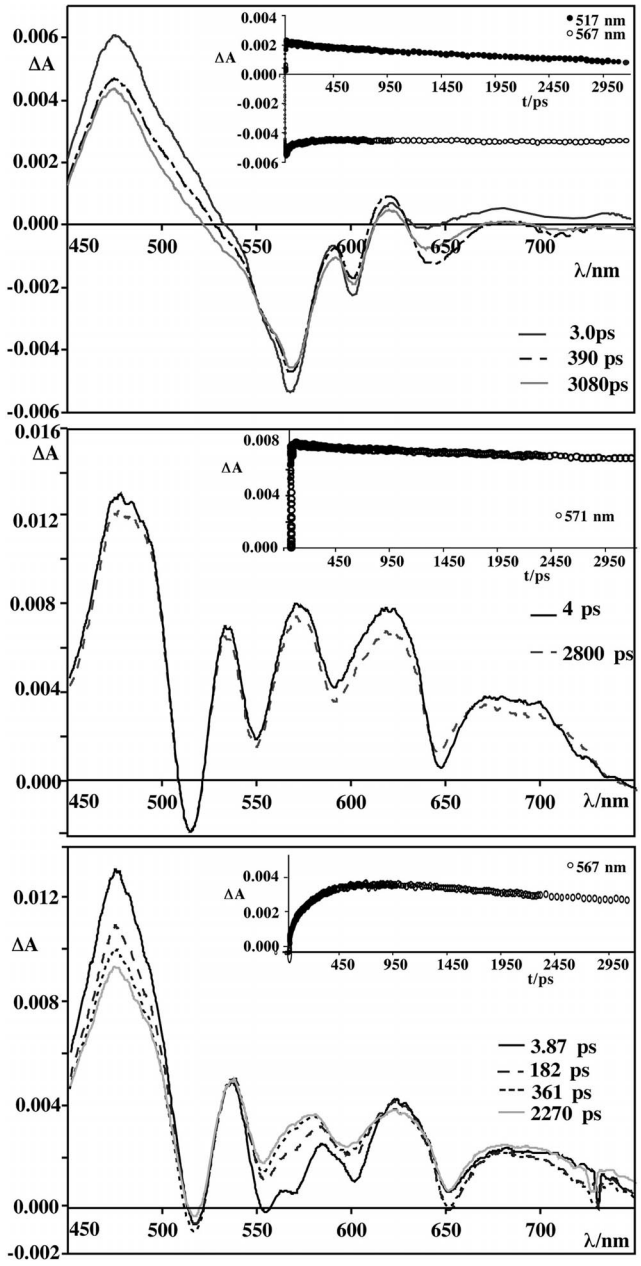

Figure 5. Transient absorption spectra (in toluene solution at room temp., excitation wavelength 400 nm at 2 mJ) of the corrole model compound **14** (top panel), the porphyrin model compound **2a** (middle panel) and dyad **6** (bottom panel). The kinetics are shown in the insets. Time delays and wavelengths at which the kinetics were studied are given in the figures.

Corrole–porphyrin dyad **6** (Figure 5, bottom panel) shows a more complicated transient spectrum. Intense transient absorption features in the visible region are present. The bleaching of the Q-bands of both the corrole and porphyrin subunits appear as "negative" contributions to the main transient absorption in the 540–650 nm region. In fact, laser excitation (400 nm) produces both corrole and porphyrin excited chromophores as selective excitation is not possible. However, in this case, the transient spectrum formed after a few picoseconds undergoes a spectral evolution during which an increased transient absorption takes place in the typical porphyrin transient absorption region (540–620 nm). The increased transient absorption is particularly evident at about 560 nm, at which there is the largest difference between the transient absorption spectra of **2a** and **14**. The risetime of such a transient is 225 (± 40 ps), assigned to the energy transfer from the singlet state of the corrole subunits to the singlet porphyrin state. Successively, the transient absorption decays with a lifetime that is close to that of **2a** (see inset of Figure 5, bottom) and is therefore assigned to the decay of the singlet state involving the porphyrin subunit of **6**. The 225 ps risetime for corrole-to-porphyrin energy transfer obtained from pump-probe spectroscopy, which corresponds to a rate constant of 4.4×10^9 s^{-1} for the energy-transfer process, is in very good agreement with the rate constant of 5×10^9 s^{-1} estimated for the same process from luminescence lifetime data (see above). To confirm this interpretation, we performed a global fitting analysis for dyad **6**. Figure 6 illustrates the result of such a fitting, which allows the main transient spectra and kinetics of the various species present in the excited state to be determined. Note, the solid curve of Figure 6 has been assigned to the transient absorption spectrum of a species that decays with a lifetime of 219 ps, and is similar to the transient spectrum of **14**, the corrole subunit of **6** (see Figure 5, top), whereas the longer-living transient spectrum (dotted curve in Figure 6) largely resembles the transient spectrum of **2a** (Figure 5, middle panel), the corresponding Fb-porphyrin building block of dyad **6**.

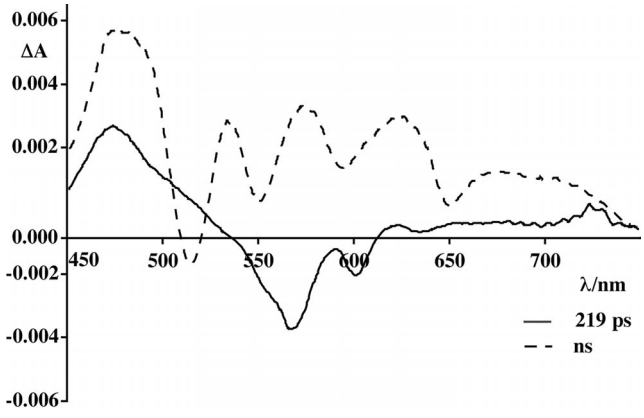

Figure 6. Transient absorption spectra of species contributing to the transient spectrum of **6** (shown in Figure 5), obtained by global kinetic analysis. The solid line is a species exhibiting a lifetime of 219 ps, the dotted line is a species with a lifetime on the ns timescale.

The situation is more complicated for tris-porphyrinoid derivative **9** as a consequence of the presence of two porphyrin subunits, the transient spectra of which tend to obscure the transient absorption of the single corrole chromophore. However, even for this multichomophoric species, the initial transient spectrum evolves, showing a biphasic decay when monitored at 567 nm (Figure 7), with a risetime of 139 (± 15) ps, followed by a transient decay on the ns timescale. The fast process has been assigned to corrole-to-porphyrin energy transfer, and a rate constant of 7.2×10^9 s^{-1} can be calculated for such an energy-transfer process, with the slower processes assigned to the decay of the porphyrin singlet state. The kinetics of the energy-transfer process are also in good agreement with the luminescence decay results (Table 1). The faster rate for the corrole-to-porphyrin singlet–singlet energy transfer in triad **9** compared with in dyad **6** is reasonable when it is considered that there are two acceptor units present in **9**, whereas only one in **6**. As a result, the probability of the process is expected to be roughly doubled in **9** compared with in **6**.

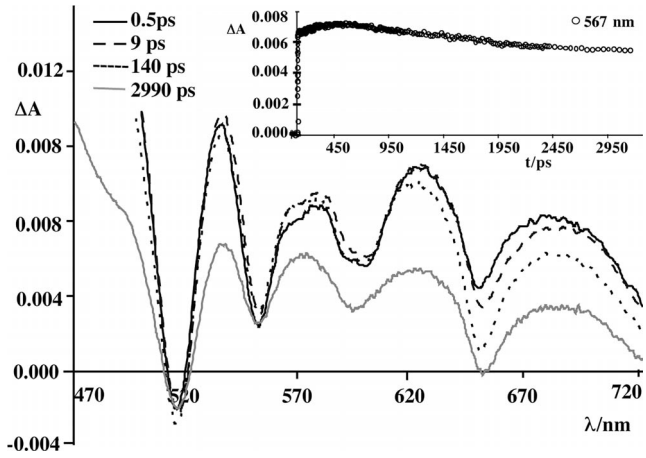

Figure 7. Transient absorption spectra (in toluene solution at room temp., excitation wavelength 400 nm at 2 mJ) of **9**. The kinetics are shown in the inset. Time delays and the wavelength at which the kinetics were studied are given in the figure.

To investigate the mechanism of the energy-transfer process, we calculated the theoretical coulombic energy-transfer rate constants by using a simplified Förster equation [Equations (1) and (2)].[22]

$$k_{en}^{F} = 8.8x10^{-25} \frac{K^2 \Phi}{n^4 r_{AB}^6 \tau} J_F \quad (1)$$

$$J_F = \frac{\int F(\bar{\nu}) \varepsilon(\bar{\nu}) / \bar{\nu}^4 \, d\bar{\nu}}{\int F(\bar{\nu}) d\bar{\nu}} \quad (2)$$

In Equation (1), $k_{en}^{F}$is the rate constant of the energy-transfer process, K is an orientation factor that accounts for the directional nature of the dipole–dipole interaction (K^2 is 2/3 for a random orientation), Φ and τ are the luminescence quantum yield and lifetime of the donor, respectively, n is the solvent refractive index (1.497 for toluene at room temp.), r_{AB} is the distance (in Å) between donor and acceptor, and J_F [see Equation (2)] is the Förster overlap integral between the luminescence spectrum of the donor, $F(\tilde{\nu})$, and the absorption spectrum of the acceptor, $\varepsilon(\tilde{\nu})$, on an energy scale (cm^{-1}). By using the spectral and kinetic values,[23] and assuming an r_{AB} through-space center-to-center distance of 13.7 Å, calculated from energy-minimized computer-generated structures, rate constants of 1.5×10^{10} and 3.2×10^{10} s^{-1} have been obtained for the corrole-to-porphyrin energy transfer in **6** and **9**, respectively. These values are larger than the experimental values by a factor of 3–4. However, by taking into account the experimental uncertainties and the approximations assumed in the Förster equation used,[24] they are in fair agreement with the experimental values and so it can be concluded that Förster energy transfer is the mechanism operating in the process observed in the corrole–porphyrin conjugates.

Note, the residual emission at 600 nm is not visible in the emission spectra of the multichromophoric species recorded at 77 K (Table 1), which can be attributed to experimental reasons. In fact, the longer excited-state lifetime of the donor(s) at 77 K coupled with the relatively high energy-transfer rate constants would result in a residual corrole-based emission <2% of the unquenched emission, probably lower than the detectable limit.

Finally, it should be noted that our results differ from the recent report of Flamigni et al. on energy transfer between Fb-corrole and -porphyrin subunits in a corrole–porphyrin dyad[7d] in which unidirectional energy transfer does not take place but rather excited-state equilibration between the two chromophoric subunits. However, in this case, the corrole unit contains two pentafluorophenyl *meso* substituents. Such substituents apparently have the effect of lowering the excited-state energy of the corrole unit so that the energy gap between the lower-lying singlet states of the corrole and porphyrin subunits is close to zero (the energy of the singlet state of the corrole unit was calculated to be less than 100 cm^{-1} higher than that of the singlet state of the porphyrin unit[7d]), so allowing for equilibration at room temperature. For the multichromophoric species investigated in this work, the energy separation between the corrole- and porphyrin-based singlet states is larger (the energy levels of the singlet states are calculated from the higher-energy feature of the corresponding emission spectra), and taking into account the relatively fast intrinsic decay of the porphyrin-based singlet (ca. 1×10^8 s^{-1}), room-temperature equilibration cannot take place.

Conclusions

meso-Pyrimidinylcorroles allow easy post-macrocyclization functionalization of the corrole scaffold, enabling the construction of (dendritic) macromolecules containing multiple porphyrinoid chromophores in an effective manner. For the first time a triad composed of an AB_2-pyrimidinylcorrole and two porphyrin units has been prepared by a straightforward nucleophilic aromatic substitution protocol and a selective metallation/demetallation procedure has been shown to afford various pyrimidinyl-bridged (heterobimetallic) corrole–porphyrin systems with readily exchangeable metal centers. Absorption spectra and photophysical features have indicated that the multichromophoric Fb-corrole–porphyrin conjugates experience only weak interchromophoric electronic interactions, which allow for fast (rate constants of about 10^9–10^{10} s^{-1}) and efficient (>95%) corrole-to-porphyrin singlet–singlet energy transfer operating by a coulombic mechanism. These systems can hence be regarded as molecular assemblies of porphyrins and corroles with supramolecular (photophysical) features and therefore represent quite realistic model systems for natural photosynthetic complexes. Future work will focus on more elaborate dendritic multiporphyrinoid systems with variable metallation states (mainly those of interest for potential photophysical applications, e.g., Ga, Ir, Al)[4c,20,25] that are capable of exhibiting tailor-made photophysical properties (e.g., a logical gradient for energy or electron transfer[26]), building on both the synthetic and photophysical knowledge gained in this study.

Experimental Section

General: NMR spectra were acquired with commercial instruments (Bruker Avance 300 MHz, AMX 400 MHz, or Avance II$^+$ 600 MHz) and chemical shifts (δ) are reported in parts per million (ppm) referenced to tetramethylsilane (^{1}H) or residual NMR solvent signals (^{13}C). Mass spectra were recorded with an ESI (Thermo Finnigan LCQ Advantage) or MALDI-TOF (Bruker Daltonics UltraFlex II TOF/TOF) mass spectrometer (with smartbeam™ laser and 2,5-dihydroxybenzoic acid matrix). High-resolution mass spectra were obtained with a Bruker Daltonics Apex2 FT-ICR mass spectrometer equipped with a combined MALDI/ESI ion source. All microwave irradiation experiments were carried out in a dedicated CEM-Discover mono-mode microwave apparatus operating at a frequency of 2.45 GHz using sealed (aluminium-Teflon® crimp-top), large (10 mL) microwave process vials. For column chromatography 70–230 mesh silica 60 (Merck) was used as the stationary phase. Chemicals received from commercial sources were used without further purification. DMF was dried with molecular sieves (4 Å). UV/Vis absorption spectra were recorded with a Jasco V-560 spectrophotometer. For steady-state luminescence measurements, a Jobin Yvon-Spex Fluoromax 2 spectrofluorimeter was used equipped with a Hamamatsu R3896 photomultiplier. The spectra were corrected for photomultiplier response by using a program purchased with the fluorimeter. For the luminescence lifetimes, an Edinburgh OB 900 time-correlated single-photon-counting spectrometer was used. A Hamamatsu PLP 2 laser diode (59 ps pulse width at 408 nm) and/or nitrogen discharge (pulse width 2 ns at 337 nm) were employed as excitation sources. Emission quantum yields for deaerated solutions were determined by the optically diluted method[27] with $[Ru(bpy)_3]^{2+}$ (bpy = 2,2′-bipyridine) in air-equilibrated aqueous solution as quantum yield standard (Φ_{em} = 0.028[28]). Time-resolved transient absorption ex-

periments were performed by using a pump-probe setup based on the Spectra-Physics MAI-TAI Ti:sapphire system as the laser source and the Ultrafast Systems Helios spectrometer as the detector. The pump pulse was generated with a Spectra-Physics 800 FP OPA instrument. The probe pulse was obtained by continuum generation on a sapphire plate (spectral range 450–800 nm). The effective time resolution was around 200 fs, and the temporal chirp over the white-light 450–750 nm range around 150 fs; the temporal window of the optical delay stage was 0–3200 ps. The time-resolved data were analyzed with the Ultrafast Systems Surface Explorer Pro software.[29] Experimental uncertainties on the absorption and photophysical data are as follows: absorption maxima, 2 nm; molar absorption, 15%; luminescence maxima, 4 nm; luminescence lifetimes, 10%; luminescence quantum yields, 20%; transient absorption decay and rise rates, 10%.

Procedures for the synthesis of pyrimidinylcorrole **1a**,[10a] its Cu-metallated counterpart **1b**,[10b] and porphyrins **2a**–**c**[11d,14] have been reported before.

Bis(Zn-Porphyrin)–Cu-Corrole Conjugate 3: A mixture of Cu-pyrimidinylcorrole **1b** (81 mg, 103 μmol), Zn-porphyrin **2b** (649 mg, 630 μmol, 6.1 equiv.), 18-crown-6 (10 mg, 38 μmol), and (finely ground) K_2CO_3 (105 mg, 760 μmol) in dry DMF (10 mL) was heated by microwave irradiation at 175 °C (100 W) for 1 h. After cooling to room temp. diethyl ether was added and the mixture was washed with distilled water. The organic fraction was dried with $MgSO_4$ and filtered. The solvent was evaporated and, after purification by column chromatography (silica, eluent CH_2Cl_2/heptane, 3:7), pure conjugate **3** (157.5 mg, 55%) was obtained as a red-brown solid together with a smaller quantity of dyad **4** (50 mg, 27%). ^{1}H NMR (300 MHz, $CDCl_3$, 25 °C, TMS): δ = 9.05–8.97 (m, 16 H, H_β porph), 8.23 [d, J(H,H) = 7.9 Hz, 4 H], 8.12 (br. s, 12 H), 8.03 (br. s, 2 H, H_β corr), 7.83–7.80 (m, 6 H), 7.72 (br. s, 2 H, H_β corr), 7.52 [d, J(H,H) = 7.9 Hz, 4 H], 7.48 (br. s, 2 H, H_β corr), 7.40 (br. s, 2 H, H_β corr), 7.05 (s, 4 H, H_{mesit}), 2.71 (s, 3 H, SMe), 2.39 (s, 6 H), 2.18 (s, 12 H), 1.55 (s, 108 H, H_{tBu}) ppm. ^{13}C NMR (100 MHz, $CDCl_3$, 25 °C, TMS): δ = 150.7, 150.6, 150.3, 148.8, 142.0, 137.8, 135.0 (CH), 132.5/132.4 (CH), 132.3, 131.7 (CH), 129.8 (CH), 128.4 (CH), 122.8, 122.7, 121.0 (CH), 120.1/119.9 (CH), 35.2, 31.9 (CH_3), 21.3 (CH_3), 20.1 (CH_3), 14.6 (SCH_3) ppm. HRMS (ESI$^+$): calcd. for $C_{178}H_{185}CuN_{14}O_2SZn_2$ 1388.1204 [M + 2H]$^{2+}$; found 1388.1233.

Zn-Porphyrin–Cu-Corrole Dyad 4: A mixture of Cu-pyrimidinylcorrole **1b** (21.7 mg, 28 μmol), Zn-porphyrin **2b** (42.6 mg, 41 μmol, 1.5 equiv.), 18-crown-6 (2 mg, 7.6 μmol), and (finely ground) K_2CO_3 (8.3 mg, 60 μmol) in dry DMF (3 mL) was heated overnight at 90 °C under Ar. After cooling to room temp. diethyl ether was added and the mixture was washed with distilled water. The organic fraction was dried with $MgSO_4$ and filtered. The solvent was evaporated and, after purification by column chromatography (silica, eluent CH_2Cl_2/heptane, 1:1), pure dyad **4** (35.3 mg, 72%) was obtained as a red-brown solid. ^{1}H NMR (300 MHz, $CDCl_3$, 25 °C, TMS): δ = 9.03–8.95 (m, 6 H, H_β porph), 8.87 [d, J(H,H) = 4.7 Hz, 2 H, H_β porph], 8.18 [d, J(H,H) = 8.3 Hz, 2 H], 8.09–8.07 (m, 6 H), 8.01 (br. s, 2 H, H_β corr), 7.80–7.77 (m, 3 H), 7.41–7.30 (m, 8 H, H_β corr, H_{Ph}), 7.05/7.03 (2 s, 4 H, H_{mesit}), 2.63 (s, 3 H, SMe), 2.39 (s, 6 H), 2.14/2.12 (2 s, 12 H), 1.52 (s, 54 H, H_{tBu}) ppm. ^{13}C NMR (100 MHz, $CDCl_3$, 25 °C, TMS): δ = 150.7, 150.6, 150.1, 148.8, 137.9, 135.0 (CH), 132.5 (CH), 129.7 (CH), 128.4 (CH), 122.7, 121.0 (CH), 119.5 (CH), 35.2, 31.9 (CH_3), 21.3 (CH_3), 20.0 (CH_3), 14.6 (SCH_3) ppm. HRMS (ESI$^+$): calcd. for $C_{110}H_{109}ClCuN_{10}OSZn$ 1779.6783 [M + H]$^+$; found 1779.6757.

Fb-Porphyrin–Cu-Corrole Dyad 5: HCl (37%, 5 drops) was added to a solution of Zn-porphyrin–Cu-corrole dyad **4** (9.4 mg, 5.3 μmol) in $CHCl_3$ (10 mL). The mixture was stirred for 10 min under Ar and diethyl ether was added. The mixture was washed with 1 M HCl followed by water until neutral. After drying of the organic fraction with $MgSO_4$ and subsequent filtration, the solvent was evaporated under reduced pressure. After flash column chromatography (silica, eluent CH_2Cl_2/heptane, 1:1), pure dyad **5** was obtained as a red-brown solid (7.1 mg, 78%). ^{1}H NMR (300 MHz, $CDCl_3$, 25 °C, TMS): δ = 8.89 (s, 4 H, H_β porph), 8.86 [d, J(H,H) = 4.9 Hz, 2 H, H_β porph], 8.75 [d, J(H,H) = 4.9 Hz, 2 H, H_β porph], 8.17 [d, J(H,H) = 8.3 Hz, 2 H], 8.07–8.04 (m, 6 H), 8.01 (br. s, 2 H, H_β corr), 7.79 (br. s, 3 H), 7.40–7.28 (m, 8 H, H_{Ph}, H_β corr), 7.05/7.02 (2 s, 4 H, H_{mesit}), 2.63 (s, 3 H, SMe), 2.39 (s, 6 H), 2.13/2.11 (2 s, 12 H), 1.51 (s, 54 H, H_{tBu}), –2.73 (br. s, 2 H, NH) ppm. HRMS (ESI$^+$): calcd. for $C_{110}H_{111}ClCuN_{10}OS$ 1717.7648 [M + H]$^+$; found 1717.7629.

Fb-Porphyrin–Fb-Corrole Dyad 6: The general Cu-corrole demetallation procedure was applied to dyad **4**.[12c] $SnCl_2{\cdot}2H_2O$ (45.2 mg, 0.2 mmol) was added to a solution of dyad **4** (33.8 mg, 19 μmol) in CH_3CN/CH_2Cl_2 (2:1; 15 mL) and the resulting mixture was stirred for 30 min at room temp. under Ar. Subsequently, concentrated aqueous HCl (1 mL) was added and stirring was continued for 30 min at room temp. under Ar. The completion of the demetallation process was monitored by ESI-MS and TLC. The mixture was diluted with diethyl ether, washed with water until neutral, dried with Na_2SO_4, and the drying agent was filtered off. The solvent was evaporated under reduced pressure and the pure Fb dyad was obtained as a purple solid in a nearly quantitative yield (31 mg, 98%) after flash column chromatography (silica, eluent CH_2Cl_2/heptane, 1:1). ^{1}H NMR (300 MHz, $CDCl_3$, 25 °C, TMS): δ = 8.88–8.81 (m, 6 H, H_β porph), 8.77 [d, J(H,H) = 4.7 Hz, 2 H, H_β porph], 8.64–8.57 (m, 6 H, H_β corr), 8.30 [d, J(H,H) = 4.1 Hz, 2 H, H_β corr], 8.10–8.00 (m, 8 H), 7.78–7.75 (m, 3 H), 7.34 [d, J(H,H) = 8.3 Hz, 2 H], 7.28/7.26 (2 s, 4 H, H_{mesit}), 2.78 (s, 3 H, SMe), 2.59 (s, 6 H), 1.98/1.96 (2 s, 12 H), 1.50/1.48 (2 s, 54 H, H_{tBu}), –2.78 (br. s, 2 H, NH) ppm. HRMS (ESI$^+$): calcd. for $C_{110}H_{114}ClN_{10}OS$ 1657.8586 [M + H]$^+$; found 1657.8624.

Zn-Porphyrin–Fb-Corrole Dyad 7: A mixture of Fb conjugate **6** (30 mg, 18 μmol) and $Zn(OAc)_2$ (10 mg, 54 μmol) in $CHCl_3$ (5 mL) was stirred at room temp. for 2 h under Ar. The solvent was evaporated under reduced pressure and, after purification by flash column chromatography (silica, eluent CH_2Cl_2/heptane, 1:1), pure Zn-porphyrin–Fb-corrole dyad **7** was obtained as a pink-purple solid (27 mg, 87%). ^{1}H NMR (300 MHz, $CDCl_3$, 25 °C, TMS): δ = 9.00–8.92 (m, 4 H, H_β), 8.88 [d, J(H,H) = 4.7 Hz, 2 H, H_β], 8.84 [d, J(H,H) = 4.1 Hz, 2 H, H_β], 8.70 [d, J(H,H) = 4.7 Hz, 2 H, H_β], 8.66–8.58 (m, 4 H, H_β), 8.30 [d, J(H,H) = 4.1 Hz, 2 H, H_β], 8.10–8.01 (m, 8 H), 7.76 (br. s, 3 H), 7.33 [d, J(H,H) = 8.3 Hz, 2 H], 7.28/7.26 (2 s, 4 H, H_{mesit}), 2.79 (s, 3 H, SMe), 2.59 (s, 6 H), 1.99/1.97 (2 s, 12 H), 1.50/1.49 (2 s, 54 H, H_{tBu}) ppm. HRMS (ESI$^+$): calcd. for $C_{110}H_{112}ClN_{10}OSZn$ 1719.7721 [M + H]$^+$; found 1719.7777.

Bis(Fb-Porphyrin)–Cu-Corrole Conjugate 8: HCl (37%, 5 drops) was added to a solution of bis(Zn-porphyrin)–Cu-corrole conjugate **3** (16.7 mg, 6 μmol) in $CHCl_3$ (10 mL). The mixture was stirred for 10 min under Ar and diethyl ether was added. The solution was washed with 1 M HCl followed by water until neutral. After drying the organic fraction with $MgSO_4$ and subsequent filtration, the solvent was evaporated under reduced pressure. After flash column chromatography (silica, eluent CH_2Cl_2/heptane, 1:1), pure conjugate **8** was obtained as a red-brown solid (10.1 mg, 63%). ^{1}H NMR (300 MHz, $CDCl_3$, 25 °C, TMS): δ = 8.91–8.80 (m, 16 H, H_β porph), 8.19 [d, J(H,H) = 8.3 Hz, 4 H], 8.09–8.02 (m, 14 H, H_{Ph},

2H_β corr), 7.81–7.77 (m, 6 H), 7.67 (br. s, 2 H, H_β corr), 7.49–7.45 (m, 6 H, H_{Ph}, 2H_β corr), 7.37 (br. s, 2 H, H_β corr), 7.04 (s, 4 H, H_{mesit}), 2.66 (s, 3 H, SMe), 2.38 (s, 6 H), 2.15 (s, 12 H), 1.53/1.52 (2 s, 108 H, H_{tBu}), –2.70 (br. s, 4 H, NH) ppm. MS (ESI$^+$): *m/z* = 2647.8 $[M + H]^+$, 1325.7 $[M + 2H]^{2+}$. HRMS (ESI$^+$): calcd. for $C_{178}H_{189}CuN_{14}O_2S$ 1325.2084 $[M + 2H]^{2+}$; found 1325.2087.

Bis(Fb-Porphyrin)–Fb-Corrole Conjugate 9: The general Cu-corrole demetallation procedure was applied to conjugate **8**.[12c] $SnCl_2{\cdot}2H_2O$ (45.2 mg, 0.2 mmol) was added to a solution of **8** (30 mg, 11 μmol) in CH_3CN/CH_2Cl_2 (2:1, 15 mL) and the resulting mixture was stirred for 30 min at room temp. under Ar. Subsequently, concentrated aqueous HCl (1 mL) was added and stirring was continued for 30 min at room temp. under Ar. The completion of the demetallation process was monitored by ESI-MS and TLC. The mixture was diluted with diethyl ether, washed with water until neutral, dried with Na_2SO_4, and the drying agent was filtered off. The solvent was evaporated under reduced pressure and the pure Fb conjugate was obtained as a purple solid in a nearly quantitative yield (28.5 mg, 97%) after flash column chromatography (silica, eluent CH_2Cl_2/heptane, 1:1). ^{1}H NMR (300 MHz, $CDCl_3$, 25 °C, TMS): δ = 9.01 [d, *J*(H,H) = 4.7 Hz, 2 H, H_β], 8.89 (s, 8 H, H_β), 8.85 [d, *J*(H,H) = 4.1 Hz, 2 H, H_β], 8.79 [d, *J*(H,H) = 4.7 Hz, 4 H, H_β], 8.73 [d, *J*(H,H) = 4.7 Hz, 2 H, H_β], 8.65 [d, *J*(H,H) = 4.9 Hz, 4 H, H_β], 8.31 [d, *J*(H,H) = 4.1 Hz, 2 H, H_β], 8.13–8.04 (m, 16 H), 7.79 (br. s, 6 H), 7.48 [d, *J*(H,H) = 8.5 Hz, 4 H], 7.27 (s, 4 H, H_{mesit}), 2.83 (s, 3 H, SMe), 2.58 (s, 6 H), 2.01 (s, 12 H), 1.52 (s, 108 H, H_{tBu}), –2.75 (br. s, 4 H, NH) ppm. HRMS (ESI$^+$): calcd. for $C_{178}H_{192}N_{14}O_2S$ 1295.2553 $[M + 2H]^{2+}$; found 1295.2518.

Bis(Zn-Porphyrin)–Fb-Corrole Conjugate 10: A mixture of Fb conjugate **9** (56 mg, 21.6 μmol) and $Zn(OAc)_2$ (20 mg, 109 μmol) in $CHCl_3$ (10 mL) was stirred at room temp. for 2 h under Ar. The solvent was evaporated under reduced pressure and, after purification by column chromatography (silica, eluent CH_2Cl_2), bis(Zn-porphyrin)–Fb-corrole conjugate **10** was obtained as a pink-purple solid in a nearly quantitative yield (57.2 mg, 97%). ^{1}H NMR (300 MHz, $CDCl_3$, 25 °C, TMS): δ = 9.02–8.97 (m, 10 H, H_β), 8.89 [d, *J*(H,H) = 4.7 Hz, 4 H, H_β], 8.85 [d, *J*(H,H) = 4.0 Hz, 2 H, H_β], 8.76 [d, *J*(H,H) = 4.5 Hz, 4 H, H_β], 8.72 [d, *J*(H,H) = 4.4 Hz, 2 H, H_β], 8.31 [d, *J*(H,H) = 3.8 Hz, 2 H, H_β], 8.12–8.03 (m, 16 H), 7.78 (br. s, 6 H), 7.47 [d, *J*(H,H) = 7.9 Hz, 4 H], 7.24 (s, 4 H, H_{mesit}), 2.83 (s, 3 H, SMe), 2.58 (s, 6 H), 2.00 (s, 12 H), 1.51 (s, 108 H, H_{tBu}) ppm. HRMS (ESI$^+$): calcd. for $C_{178}H_{188}N_{14}O_2SZn_2$ 1358.1673 $[M + 2H]^{2+}$; found 1358.1666.

Bis(Zn-Porphyrin)–Ga-Corrole Conjugate 11: A large excess of $GaCl_3$ (0.5 M in pentane, 2 mL) was added to a solution of bis(Zn-porphyrin)–Fb-corrole conjugate **10** (7.5 mg, 2.8 μmol) in pyridine (5 mL). The solution was stirred at reflux for 1 h under Ar and then the pyridine was evaporated under reduced pressure. After purification by column chromatography (silica, eluent CH_2Cl_2/heptane/pyridine, 3:2:0.02), pure bis(Zn-porphyrin)–Ga-corrole conjugate **11** (6.0 mg, 76%) was obtained as a purple-green solid. ^{1}H NMR (600 MHz, $CDCl_3$, 25 °C, TMS): δ = 9.06–9.02 (m, 4 H, H_β), 8.99–8.93 (m, 8 H, H_β), 8.88 [d, *J*(H,H) = 4.5 Hz, 4 H, H_β], 8.81 [d, *J*(H,H) = 4.5 Hz, 2 H, H_β], 8.76 [d, *J*(H,H) = 4.5 Hz, 4 H, H_β], 8.57 [d, *J*(H,H) = 3.8 Hz, 2 H, H_β], 8.08 [d, *J*(H,H) = 8.3 Hz, 4 H, H_{Ph}], 8.06–8.03 (m, 12 H), 7.77 (br. s, 6 H), 7.43 [d, *J*(H,H) = 7.9 Hz, 4 H, H_{Ph}], 7.25 (s, 4 H, H_{mesit}), 6.72–6.67 (m, 1 H, $H_{p\text{-pyrid}}$), 5.89–5.84 (m, 2 H, $H_{m\text{-pyrid}}$), 3.54 (br. s, 2 H, $H_{o\text{-pyrid}}$), 2.82 (s, 3 H, SMe), 2.59 (s, 6 H), 1.92 (br. s, 12 H), 1.51/1.50 (2 s, 108 H, H_{tBu}) ppm. MS (MALDI-TOF): calcd. for $C_{178}H_{183}GaN_{14}O_2SZn_2$ 2780.2 [M – pyridine]$^+$; found 2780.1.

Bis(Pt-Porphyrin)–Cu-Corrole Conjugate 12: A mixture of Cu-pyrimidinylcorrole **1b** (5.1 mg, 6.5 μmol), Pt-porphyrin **2c** (45 mg, 39 μmol, 6 equiv.), 18-crown-6 (1 mg, 4 μmol), and (finely ground) K_2CO_3 (6 mg, 43 μmol) in dry DMF (3 mL) was heated by microwave irradiation at 165 °C (100 W) for 1 h. After cooling to room temp. diethyl ether was added and the mixture was washed with distilled water. The organic fraction was dried with $MgSO_4$ and filtered. The solvent was evaporated and, after purification by column chromatography (silica, eluent CH_2Cl_2/heptane, 3:7), pure triad **12** (14 mg, 73%) was obtained as an orange-brown solid. ^{1}H NMR (400 MHz, $CDCl_3$, 25 °C, TMS): δ = 8.82–8.71 (m, 16 H, H_β), 8.11 [d, *J*(H,H) = 8.0 Hz, 4 H], 8.01 (br. s, 14 H, H_{Ph}, 2H_β), 7.78 (br. s, 6 H), 7.63 (br. s, 2 H, H_β), 7.47–7.42 (m, 6 H, H_{Ph}, 2 H_β), 7.36 (br. s, 2 H, H_β corr), 7.04 (s, 4 H, H_{mesit}), 2.63 (s, 3 H, SMe), 2.38 (s, 6 H), 2.14 (s, 12 H), 1.51/1.50 (s, 108 H, H_{tBu}) ppm. MS (MALDI-TOF): calcd. for $C_{178}H_{183}CuN_{14}O_2Pt_2S$ 3033.3 $[M]^+$; found 3033.5.

Pt-Porphyrin–Cu-Corrole Dyad 13: A mixture of Cu-pyrimidinylcorrole **1b** (15 mg, 19 μmol), Pt-porphyrin **2c** (25 mg, 22 μmol, 1.2 equiv.), 18-crown-6 (1 mg, 4 μmol), and (finely ground) K_2CO_3 (4.5 mg, 33 μmol) in dry DMF (5 mL) was heated overnight at 90 °C under Ar. After cooling to room temp. diethyl ether was added and the mixture was washed with distilled water. The organic fraction was dried with $MgSO_4$ and subsequently filtered. The solvent was evaporated and, after purification by column chromatography (silica, eluent CH_2Cl_2/heptane, 7:3), pure dyad **13** (6.3 mg, 19%) was obtained as an orange-brown solid. ^{1}H NMR (300 MHz, $CDCl_3$, 25 °C, TMS): δ = 8.82–8.73 (m, 6 H, H_β), 8.65 [d, *J*(H,H) = 5.1 Hz, 2 H, H_β], 8.10 [d, *J*(H,H) = 8.3 Hz, 2 H], 8.01–7.98 (m, 8 H, 2H_β, H_{Ph}), 7.77 (br. s, 3 H), 7.38–7.25 (m, 8 H, 6 H_β, H_{Ph}), 7.05/7.02 (2 s, 4 H, H_{mesit}), 2.61 (s, 3 H, SMe), 2.39 (s, 6 H), 2.13/2.11 (2 s, 12 H), 1.50 (s, 54 H, H_{tBu}) ppm. HRMS (ESI$^+$): calcd. for $C_{110}H_{109}ClCuN_{10}OPtS$ 1910.7139 $[M + H]^+$; found 1910.7209.

Supporting Information (see footnote on the first page of this article): NMR spectra (^{1}H, ^{13}C) of corrole–porphyrin conjugates **3**–**13** and selected (high-resolution) mass spectra.

Acknowledgments

The authors thank the Institute for the Promotion of Innovation through Science and Technology in Flanders (IWT) and the Alexander von Humboldt Foundation for a doctoral and postdoctoral fellowship, respectively, to T. H. N., the Fund for Scientific Research - Flanders (FWO) for financial support and a postdoctoral fellowship to W. M., and the KU Leuven and the Ministerie voor Wetenschapsbeleid for continuing financial support. The University of Messina (Progetti di Ricerca di Ateneo and Fondi per Giovani Ricercatori) and Ministero dell'Università e della Ricerca (MIUR) (PRIN contract number 20085ZXFEE and FIRB RBAP11C58Y, "NanoSolar") are also acknowledged for financial support.

[1] a) A. W. Johnson, R. Price, *J. Chem. Soc.* **1960**, 1649–1653; b) A. W. Johnson, I. T. Kay, *Proc. Chem. Soc.* **1961**, 168–169; c) A. W. Johnson, I. T. Kay, *J. Chem. Soc.* **1965**, 1620–1629.

[2] a) E. Rose, A. Kossanyi, M. Quelquejeu, M. Soleilhavoup, F. Duwavran, N. Bernard, A. Lecas, *J. Am. Chem. Soc.* **1996**, *118*, 1567–1568; b) Z. Gross, N. Galili, I. Saltsman, *Angew. Chem.* **1999**, *111*, 1530–1533; *Angew. Chem. Int. Ed.* **1999**, *38*, 1427–1429; c) Z. Gross, N. Galili, L. Simkhovich, I. Saltsman, N. Botoshansky, D. Bläser, R. Boese, I. Goldberg, *Org. Lett.* **1999**, *1*, 599–602; d) R. Paolesse, L. Jaquinod, D. J. Nurco, S. Mini,

F. Sagone, T. Boschi, K. M. Smith, *Chem. Commun.* **1999**, 1307–1308; e) D. T. Gryko, *Chem. Commun.* **2000**, 2243–2244; f) B. Koszarna, D. T. Gryko, *J. Org. Chem.* **2006**, *71*, 3707–3717.

[3] For reviews on (synthetic) corrole chemistry, see: a) D. T. Gryko, *Eur. J. Org. Chem.* **2002**, 1735–1742; b) D. T. Gryko, J. P. Fox, P. Goldberg, *J. Porphyrins Phthalocyanines* **2004**, *8*, 1091–1105; c) A. Ghosh, *Angew. Chem.* **2004**, *116*, 1952–1965; *Angew. Chem. Int. Ed.* **2004**, *43*, 1918–1931; d) S. Nardis, D. Monti, R. Paolesse, *Mini-Rev. Org. Chem.* **2005**, *2*, 355–372; e) R. Paolesse, *Synlett* **2008**, 2215–2230; f) D. T. Gryko, *J. Porphyrins Phthalocyanines* **2008**, *12*, 906–917; g) C. M. Lemon, P. J. Brothers, *J. Porphyrins Phthalocyanines* **2011**, *15*, 809–834.

[4] a) J.-M. Barbe, G. Canard, S. Brandès, R. Guilard, *Chem. Eur. J.* **2007**, *13*, 2118–2129; b) I. Aviv, Z. Gross, *Chem. Commun.* **2007**, 1987–1999; c) L. Flamigni, D. T. Gryko, *Chem. Soc. Rev.* **2009**, *38*, 1635–1646; d) I. Aviv-Harel, Z. Gross, *Chem. Eur. J.* **2009**, *15*, 8382–8394; e) A. Kanamori, M.-M. Catrinescu, A. Mahammed, Z. Gross, L. A. Levin, *J. Neurochem.* **2010**, *114*, 488–498; f) J. Y. Hwang, J. Lubow, D. Chu, J. Ma, H. Agadjanian, J. Sims, H. B. Gray, Z. Gross, D. L. Farkas, L. K. Medina-Kauwe, *Mol. Pharm.* **2011**, *8*, 2233–2243; g) D. K. Dogutan, R. McGuire Jr, D. G. Nocera, *J. Am. Chem. Soc.* **2011**, *133*, 9178–9180; h) I. Aviv-Harel, Z. Gross, *Coord. Chem. Rev.* **2011**, *255*, 717–736.

[5] a) R. Paolesse, R. K. Pandey, T. P. Forsyth, L. Jaquinod, K. R. Gerzevske, D. J. Nurco, M. O. Senge, S. Licoccia, T. Boschi, K. M. Smith, *J. Am. Chem. Soc.* **1996**, *118*, 3869–3882; b) R. Paolesse, F. Sagone, A. Macagnano, T. Boschi, L. Prodi, M. Montalti, N. Zaccheroni, F. Bolletta, K. M. Smith, *J. Porphyrins Phthalocyanines* **1999**, *3*, 364–370.

[6] a) F. Jérôme, C. P. Gros, C. Tardieux, J.-M. Barbe, R. Guilard, *New J. Chem.* **1998**, *22*, 1327–1329; b) F. Jérôme, C. P. Gros, C. Tardieux, J.-M. Barbe, R. Guilard, *Chem. Commun.* **1998**, 2007–2008; c) K. M. Kadish, Z. Ou, J. Shao, C. P. Gros, J.-M. Barbe, F. Jérôme, F. Bolze, F. Burdet, R. Guilard, *Inorg. Chem.* **2002**, *41*, 3990–4005; d) J.-M. Barbe, G. Morata, E. Espinosa, R. Guilard, *J. Porphyrins Phthalocyanines* **2003**, *7*, 120–124; e) J.-M. Barbe, F. Burdet, E. Espinosa, C. P. Gros, R. Guilard, *J. Porphyrins Phthalocyanines* **2003**, *7*, 365–374; f) J.-M. Barbe, F. Burdet, E. Espinosa, R. Guilard, *Eur. J. Inorg. Chem.* **2005**, 1032–1041; g) R. Guilard, F. Burdet, J.-M. Barbe, C. P. Gros, E. Espinosa, J. Shao, Z. Ou, R. Zhan, K. M. Kadish, *Inorg. Chem.* **2005**, *44*, 3972–3983; h) K. M. Kadish, L. Frémond, F. Burdet, J.-M. Barbe, C. P. Gros, R. Guilard, *J. Inorg. Biochem.* **2006**, *100*, 858–868; i) J. Poulin, C. Stern, R. Guilard, P. D. Harvey, *Photochem. Photobiol.* **2006**, *82*, 171–176; j) C. P. Gros, F. Brisach, A. Meristoudi, E. Espinosa, R. Guilard, P. D. Harvey, *Inorg. Chem.* **2007**, *46*, 125–135; k) P. Chen, M. El Ojaimia, C. P. Gros, J.-M. Barbe, R. Guilard, J. Shen, K. M. Kadish, *J. Porphyrins Phthalocyanines* **2011**, *15*, 188–198.

[7] a) S. Hiroto, I. Hisaki, H. Shinokubo, A. Osuka, *Angew. Chem.* **2005**, *117*, 6921–6924; *Angew. Chem. Int. Ed.* **2005**, *44*, 6763–6766; b) S. Hiroto, K. Furukawa, H. Shinokubo, A. Osuka, *J. Am. Chem. Soc.* **2006**, *128*, 12380–12381; c) J. F. B. Barata, A. M. G. Silva, M. G. P. M. S. Neves, A. C. Tomé, A. M. S. Silva, J. A. S. Cavaleiro, *Tetrahedron Lett.* **2006**, *47*, 8171–8174; d) L. Flamigni, B. Ventura, M. Tasior, D. T. Gryko, *Inorg. Chim. Acta* **2007**, *360*, 803–813; e) B. Koszarna, D. T. Gryko, *Chem. Commun.* **2007**, 2994–2996.

[8] R. Ruppert, C. Jeandon, H. J. Callot, *J. Org. Chem.* **2008**, *73*, 694–700.

[9] Occasionally observed μ-oxo dimers have been excluded from this overview.

[10] a) W. Maes, T. H. Ngo, J. Vanderhaeghen, W. Dehaen, *Org. Lett.* **2007**, *9*, 3165–3168; b) T. H. Ngo, F. Puntoriero, F. Nastasi, K. Robeyns, L. Van Meervelt, S. Campagna, W. Dehaen, W. Maes, *Chem. Eur. J.* **2010**, *16*, 5691–5705; c) T. H. Ngo, F. Nastasi, F. Puntoriero, S. Campagna, W. Dehaen, W. Maes, *J. Org. Chem.* **2010**, *75*, 2127–2130; d) F. Nastasi, S. Campagna, T. H. Ngo, W. Dehaen, W. Maes, M. Kruk, *Photochem. Photobiol. Sci.* **2011**, *10*, 143–150.

[11] a) W. Maes, W. Dehaen, *Synlett* **2003**, 79–82; b) W. Maes, D. B. Amabilino, W. Dehaen, *Tetrahedron* **2003**, *59*, 3937–3943; c) W. Maes, J. Vanderhaeghen, W. Dehaen, *Chem. Commun.* **2005**, 2612–2614; d) W. Maes, J. Vanderhaeghen, S. Smeets, C. V. Asokan, L. M. Van Renterghem, F. E. Du Prez, M. Smet, W. Dehaen, *J. Org. Chem.* **2006**, *71*, 2987–2994; e) W. Maes, W. Dehaen, *Pol. J. Chem.* **2008**, *82*, 1145–1160; f) T. H. Ngo, K. A. Nitychoruk, D. Lentz, T. Rzymowski, W. Dehaen, W. Maes, *Tetrahedron Lett.* **2012**, *53*, 2406–2409.

[12] a) F. Mandoj, S. Nardis, G. Pomarico, R. Paolesse, *J. Porphyrins Phthalocyanines* **2008**, *12*, 19–26; b) C. Capar, K. E. Thomas, A. Ghosh, *J. Porphyrins Phthalocyanines* **2008**, *12*, 964–967; c) T. H. Ngo, W. Van Rossom, W. Dehaen, W. Maes, *Org. Biomol. Chem.* **2009**, *7*, 439–443.

[13] T. Rohand, E. Dolusic, T. H. Ngo, W. Maes, W. Dehaen, *ARKIVOC* **2007**, 307–324.

[14] H. Yamada, H. Imahori, S. Fukuzumi, *J. Mater. Chem.* **2002**, *12*, 2034–2040.

[15] For a review on porphyrin dendrimers, see: W. Maes, W. Dehaen, *Eur. J. Org. Chem.* **2009**, 4719–4752.

[16] M. Pittelkow, T. Brock-Nannestad, J. Bendix, J. B. Christensen, *Inorg. Chem.* **2011**, *50*, 5867–5869.

[17] A. Mahammed, Z. Gross, *J. Inorg. Biochem.* **2002**, *88*, 305–309.

[18] J. W. Buchler, K.-L. Lay, H. Stoppa, *Z. Naturforsch. B* **1980**, *35*, 433–438.

[19] J. Bendix, I. J. Dmochowski, H. B. Gray, A. Mahammed, L. Simkhovich, Z. Gross, *Angew. Chem.* **2000**, *112*, 4214–4217; *Angew. Chem. Int. Ed.* **2000**, *39*, 4048–4051.

[20] For previous studies on corrole photophysics, see: a) A. Ghosh, T. Wondimagegn, A. B. J. Parusel, *J. Am. Chem. Soc.* **2000**, *122*, 6371–6374; b) R. Paolesse, A. Marini, S. Nardis, A. Froiio, F. Mandoj, D. J. Nurco, L. Prodi, M. Montalti, K. M. Smith, *J. Porphyrins Phthalocyanines* **2003**, *7*, 25–26; c) T. Ding, J. D. Harvey, C. J. Ziegler, *J. Porphyrins Phthalocyanines* **2005**, *9*, 22–27; d) T. Ding, E. A. Aleman, D. A. Modarelli, C. J. Ziegler, *J. Phys. Chem. A* **2005**, *109*, 7411–7417; e) B. Ventura, A. Degli Esposti, B. Koszarna, D. T. Gryko, L. Flamigni, *New J. Chem.* **2005**, *29*, 1559–1566; f) M. Tasior, D. T. Gryko, M. Cembor, J. S. Jaworski, B. Ventura, L. Flamigni, *New J. Chem.* **2007**, *31*, 247–259; g) L. Flamigni, M. Ventura, M. Tasior, T. Becherer, H. Langhals, D. T. Gryko, *Chem. Eur. J.* **2008**, *14*, 169–183; h) F. D'Souza, R. Chitta, K. Ohkubo, M. Tasior, N. K. Subbaiyan, M. E. Zandler, M. K. Rogacki, D. T. Gryko, S. Fukuzumi, *J. Am. Chem. Soc.* **2008**, *130*, 14263–14272; i) M. Tasior, D. T. Gryko, J. Shen, K. M. Kadish, T. Becherer, H. Langhals, B. Ventura, L. Flamigni, *J. Phys. Chem. C* **2008**, *112*, 19699–19709; j) L. Shi, H.-Y. Liu, H. Shen, J. Hu, G.-L. Zhang, H. Wang, L.-N. Ji, C.-K. Chang, H.-F. Jiang, *J. Porphyrins Phthalocyanines* **2009**, *13*, 1221–1226; k) L. L. You, H. Shen, L. Shi, G. L. Zhang, H. Y. Liu, H. Wang, L. N. Ji, *Sci. China Ser. G* **2010**, *53*, 1491–1496; l) M. Tasior, D. T. Gryko, D. J. Pielacinska, A. Zanelli, L. Flamigni, *Chem. Asian J.* **2010**, *5*, 130–140; m) L. Shi, H.-Y. Liu, K.-M. Peng, X.-L. Wang, L.-L. You, J. Lu, L. Zhang, H. Wang, L.-N. Ji, H.-F. Jiang, *Tetrahedron Lett.* **2010**, *51*, 3439–3442; n) L. Flamigni, D. Wyrostek, R. Voloshchuk, D. Gryko, *Phys. Chem. Chem. Phys.* **2010**, *12*, 474–483; o) L. Flamigni, A. I. Ciuciu, H. Langhals, B. Böck, D. T. Gryko, *Chem. Asian J.* **2012**, *7*, 582–592; see also refs.[4c,5b,6i,6j,7d,7e,10b,10d].

[21] K. M. Kadish, K. M. Smith, R. Guilard (Eds.), *Handbook of Porphyrin Science*, vol. 1, Imperial College Press, London, **2010**.

[22] Th. Förster, *Discuss. Faraday Soc.* **1959**, *27*, 7–17.

[23] For the donor emission, we used the room-temperature emission spectra of **14** and **15** to calculate the rate constants of **6** and **9**, respectively; donor lifetimes and quantum yields were obtained from model corroles **14** and **15**. The acceptor absorption spectrum is similar to that of **2a**. For **9**, the value of ε for

the acceptor is considered to be twice that of **6**, taking into account the presence of two equivalent porphyrin units.

[24] Among other factors, small differences in the emission spectra, lifetimes and quantum yields of the effective corrole components in the multichromophoric species with respect to the values derived from the models could account for the differences between the energy-transfer rate constants calculated by using the Förster equation and experimentally measured values.

[25] a) D. Kowalska, X. Liu, U. Tripathy, A. Mahammed, Z. Gross, S. Hirayama, R. P. Steer, *Inorg. Chem.* **2009**, *48*, 2670–2676; b) J. H. Palmer, A. C. Durrell, Z. Gross, J. R. Winkler, H. B. Gray, *J. Am. Chem. Soc.* **2010**, *132*, 9230–9231; c) J. Vestfrid, M. Botoshansky, J. H. Palmer, A. C. Durrell, H. B. Gray, Z. Gross, *J. Am. Chem. Soc.* **2011**, *133*, 12899–12901; d) Y. Yang, D. Jones, T. von Haimberger, M. Linke, L. Wagnert, A. Berg, H. Levanon, A. Zacarias, A. Mahammed, Z. Gross, K. Heyne, *J. Phys. Chem. A* **2012**, *116*, 1023–1029.

[26] L. Le Pleux, Y. Pellegrin, E. Blart, F. Odobel, A. Harriman, *J. Phys. Chem. A* **2011**, *115*, 5069–5080.

[27] J. N. Demas, G. A. Crosby, *J. Phys. Chem.* **1971**, *75*, 991–1024.

[28] K. Nakamaru, *Bull. Chem. Soc. Jpn.* **1982**, *55*, 2697–2705.

[29] http://www.ultrafastsystems.com/surfexp.html.

Received: June 22, 2012
Published Online: ■

Porphyrinoid Multichromophores

Corrole–porphyrin multichromophoric systems containing a variety of (readily exchangeable) metals in the tetrapyrrolic ligands have been successfully synthesized starting from a versatile *meso*-pyrimidinylcorrole scaffold. Although the conjugates show only weak interchromophoric electronic interactions, fast and efficient corrole-to-porphyrin singlet–singlet energy transfer was observed.

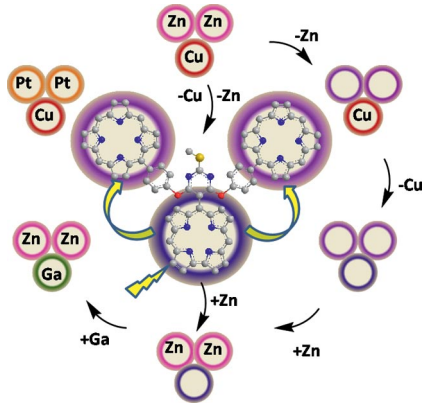

Keywords: Porphyrinoids / Macromolecules / Energy transfer / Chromophores / UV/Vis spectroscopy

